

PAPER

# Texture analysis of ultra-high coercivity $\text{Sm}_2\text{Co}_7$ hot deformation magnets\*

To cite this article: Qiang Ma *et al* 2021 *Chinese Phys. B* **30** 047505

View the [article online](#) for updates and enhancements.

## You may also like

- [Sm–Co high-temperature permanent magnet materials](#)  
Shiqiang Liu and
- [Facile Electrochemical Preparation of Al–Sm Alloys in Molten Calcium Chloride](#)  
Junfeng Li, Mingyong Wang, Jiguo Tu et al.
- [Magnetic Behaviour of  \$\text{Sm}\_2\text{Co}\_7/\text{Fe}/\text{Sm}\_2\text{Co}\_7\$  Nanocomposite Trilayers with Cr and Ti Additions](#)  
F. Shahzad, S. A. Siddiqi and J. Zhou

# Texture analysis of ultra-high coercivity $\text{Sm}_2\text{Co}_7$ hot deformation magnets\*

Qiang Ma(马强)<sup>1,2,3</sup>, Meishuang Jia(贾美爽)<sup>2</sup>, Zhifeng Hu(胡智峰)<sup>2</sup>, Ming Yue(岳明)<sup>3</sup>, Yanli Liu(刘艳丽)<sup>1,2</sup>, Tongyun Zhao(赵同云)<sup>1</sup>, and Baogen Shen(沈保根)<sup>1,†</sup>

<sup>1</sup>State Key Laboratory of Magnetism, Institute of Physics, Chinese Academy of Sciences, Beijing 100190, China

<sup>2</sup>School of Science, Inner Mongolia University of Science and Technology, Baotou 014010, China

<sup>3</sup>College of Materials Science and Engineering, Beijing University of Technology, Beijing 100124, China

(Received 15 December 2020; revised manuscript received 20 January 2021; accepted manuscript online 4 February 2021)

Bulk anisotropic  $\text{Sm}_2\text{Co}_7$  nanocrystalline magnets were successfully prepared by hot deformation process using spark plasma sintering technology. The coercivity of the isotropic  $\text{Sm}_2\text{Co}_7$  nanocrystalline magnet is 34.76 kOe, further, the ultra-high coercivity of 50.68 kOe is obtained in the anisotropic hot deformed  $\text{Sm}_2\text{Co}_7$  magnet when the height reduction is 70%, which is much higher than those of the ordinarily produced hot deformed  $\text{Sm}_2\text{Co}_7$  magnet. X-ray diffraction (XRD) analysis shows that all the samples are  $\text{Sm}_2\text{Co}_7$  single phase. The investigation by electron backscatter diffraction indicates that increasing the amount of deformation is beneficial to the improvement of the (001) texture of  $\text{Sm}_2\text{Co}_7$  magnets. The  $\text{Sm}_2\text{Co}_7$  nanocrystalline magnet generates a strong *c*-axis crystallographic texture during large deformation process.

**Keywords:**  $\text{Sm}_2\text{Co}_7$  magnet, spark plasma sintering, hot deformation, ultra-high coercivity, texture

**PACS:** 75.47.Np, 75.50.Ww, 75.60.Jk

**DOI:** 10.1088/1674-1056/abe2fc

## 1. Introduction

Sm–Co alloys such as  $\text{SmCo}_5$ ,  $\text{Sm}_2\text{Co}_{17}$ , and  $\text{SmCo}_7$  have been extensively studied for high Curie temperature ( $T_C$ ) and large magnetocrystalline anisotropy ( $H_A$ ).<sup>[1–7]</sup>  $\text{Sm}_2\text{Co}_7$  is a kind of magnet with great potential for use in high temperature environment due to its large  $H_A$  ( $> 200$  kOe) and good phase stability.<sup>[8–12]</sup> With the development of nanotechnology and the application of spark plasma sintering (SPS) technology in the field of nanocrystalline magnet preparation, the preparation of ultra-high coercivity ( $H_{cj}$ ) Sm–Co bulk magnets becomes possible.<sup>[13]</sup> Preparation of Sm–Co alloy magnets by using SPS process can effectively avoid the abnormal growth of crystal grains and provide high coercivity.<sup>[14–16]</sup> Coercivity and phase stability of  $\text{Sm}_2\text{Co}_7$  type nanocrystalline magnets have been reported, but few studies have focused on the  $\text{Sm}_2\text{Co}_7$  anisotropic magnet.<sup>[17,18]</sup> Magnetic performance of isotropic nanocrystalline  $\text{Sm}_2\text{Co}_7$  is not high enough due to its low magnetic orientation. Hot deformation process is an effective method to obtain magnetic anisotropy of nanocrystalline magnets. However, strong *c*-axis crystallographic texture has never been reported so far for  $\text{Sm}_2\text{Co}_7$  nanocrystalline magnet. The present work is aimed to prepare  $\text{Sm}_2\text{Co}_7$  anisotropic magnet with strong texture by means of hot pressing and hot deformation, and to study the formation mechanism of the texture.

## 2. Experimental procedures

The  $\text{Sm}_2\text{Co}_7$  alloy ingots with a stoichiometric ratio 2:7 (at.%) were prepared by induction melting of elemental Sm and Co both with 99.95% purity under the purified argon atmosphere. An excess of 5 wt.% Sm was used to compensate for its losses during the preparation. The ingots were quenched into ribbons at a wheel speed of 30 m/s and then high energy ball milled into amorphous powders. The powders were hot pressed (HP) at 700 °C with a pressure of 450 MPa. In order to obtain anisotropic magnets, the isotropic hot pressed magnets were hot deformed (HD) with height reductions of 70%, 80%, and 90% (named HD70%, HD80%, and HD90%, respectively) at the temperature of 720–750 °C under the pressure of 20–50 kN. The magnetic properties of the samples were measured by vibrating sample magnetometer (VSM). X-ray diffraction (XRD) measurement of the hot pressed and hot deformed samples has been performed by using  $\text{Co } K\alpha$  radiation. Electron backscatter diffraction (EBSD) was carried out to analyze the orientation and the mechanism of the texture formation. All of the test surfaces of the samples were perpendicular to the direction of pressure.

## 3. Results and discussion

As shown in Fig. 1, the coercivity  $H_{cj}$  of the isotropic  $\text{Sm}_2\text{Co}_7$  HP magnet is 34.76 kOe, the remanence  $M_r$  is

\*Project supports by the Science Center of the National Natural Science Foundation of China (Grant No. 52088101), the National Natural Foundation of China (Grant No. 51590880), the Fujian Institute of Innovation, Chinese Academy of Sciences (Grant No. FJXCXY18040302), the Key Program of the Chinese Academy of Sciences (Grant No. KJZD-EW-M05-1), and the Natural Science Foundation of Inner Mongolia, China (Grant Nos. 2018LH05006 and 2018LH05011).

†Corresponding author. E-mail: shenbg@iphy.ac.cn

36.23 emu/g, and the maximum energy product  $(BH)_{\max}$  is 3.76 MGOe. The sample of HD70% exhibits a coercivity as high as 50.68 kOe, which is the highest coercivity that SmCo bulk magnet has ever been reported to possess, and the remanence is 40.05 emu/g. As the die upset level increases to 80%, the coercivity of the magnet still remains 32.32 kOe, and the remanence increases to 48.56 emu/g. For the HD90% sample, the coercivity is drastically reduced to 4.60 kOe, while the remanence is increased to 63.10 emu/g and the maximum energy product is 8.21 MGOe. With the increase of height reduction, the increases of magnetic remanence and magnetic energy product arise from the enhancement of the magnetic anisotropy. The details of the magnetic properties of the Sm<sub>2</sub>Co<sub>7</sub> HP and HD magnets are shown in Table 1. The orientation degree of the magnet was calculated by the value of  $M_r/M_s$  ( $M_s$  is the saturation magnetization at the magnetic field of 70 kOe). It is found that with the increase of the die upset level, the value of  $M_r/M_s$  is increased from 82.20% to 94.74%, indicating that the orientation of  $c$ -axis of the magnets is optimized.<sup>[15]</sup>

The result of the Sm<sub>2</sub>Co<sub>7</sub> magnet HP sample analyzed using XRD is shown in Fig. 2 by black line. As seen in the pattern, the magnet has a Sm<sub>2</sub>Co<sub>7</sub> single phase with a hexagonal Ce<sub>2</sub>Ni<sub>7</sub>-type structure (PDF# 71-0387) at the room temperature. Figure 2 also shows the XRD patterns of the hot-deformed Sm<sub>2</sub>Co<sub>7</sub> magnets. As the die upset level increases, the peak of (00 12) is continually rising while the peak of (116) decreases, which means that the Sm<sub>2</sub>Co<sub>7</sub> grains have a preferred orientation during the HD process, resulting in a (001) texture. The texture strength is quantitatively characterized by the value of  $I_{(00\ 12)}/I_{(116)}$ . The  $I_{(00\ 12)}/I_{(116)}$  of the HP magnet is 0.53, then, with the amount of die upset level increased by 90%, the value of  $I_{(00\ 12)}/I_{(116)}$  reaches 6.93, which is 13.08

times higher than that of HP magnet. The strong  $c$ -axis texture of the HD90% magnet is the reason for the high value of  $M_r/M_s$  and high  $M_r$  in Table 1.

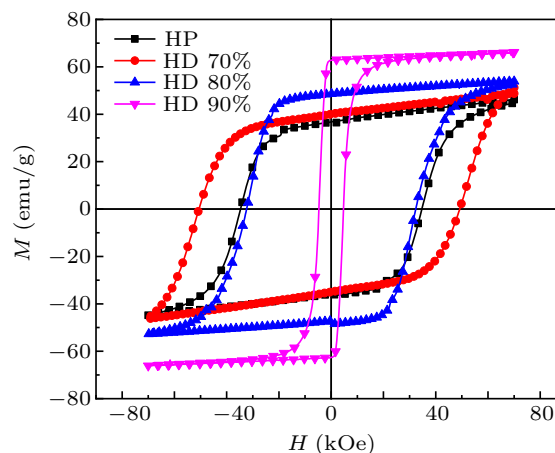


Fig. 1. Hysteresis loop of the Sm<sub>2</sub>Co<sub>7</sub> HP and HD magnets.

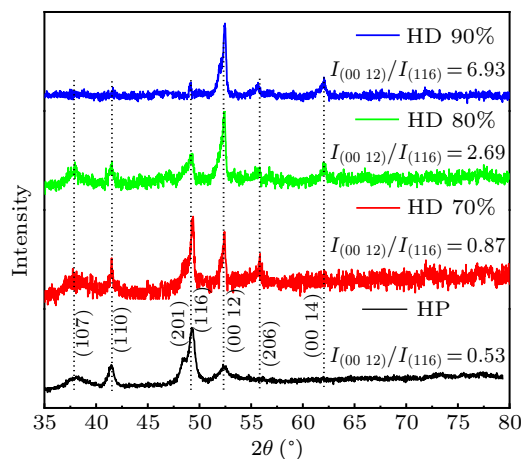


Fig. 2. XRD patterns of the HP and HD Sm<sub>2</sub>Co<sub>7</sub> magnets.

Table 1. Magnetic properties of the hot-pressed and hot-deformed Sm<sub>2</sub>Co<sub>7</sub> magnets.

Sample	$H_{c1}$ (kOe)	$M_r$ (emu/g)	$M_s(70\text{ kOe})$ (emu/g)	$(BH)_{\max}$ (MGOe)	$M_r/M_s$	$\rho$ (g/cm <sup>3</sup> )
HP	34.76	36.23	46.12	3.76	78.56%	8.41
HD 70%	50.68	40.05	48.72	4.47	82.20%	8.52
HD 80%	32.32	48.56	54.46	6.65	89.17%	8.51
HD 90%	4.60	63.10	66.60	8.21	94.74%	8.54

The magnets densities were tested using the Archimedes principle. As shown in Table 1, the density of the magnets after HD process is higher than that of the HP magnet, which indicates that some defects disappear in a long period of high temperature deformation during the HD process. As shown in Fig. 3(a), the grain size of the HD 70% Sm<sub>2</sub>Co<sub>7</sub> magnet is about 300 nm, the grain boundaries are clearly visible, and the size of the grain is uniform, which are the reasons for obtaining ultra-high coercivity. In Fig. 3(b), when the amount of the height reduction increases to 80%, the grains grow to 800 nm in size, which decreases the coercivity. The further growth of

grains in the HD 90% samples results in the distribution of some micron-sized grains in the magnets, leading to the rapid decline of coercivity.

The orientation texture and microstructure of the HD Sm<sub>2</sub>Co<sub>7</sub> magnets were characterized by electron backscatter diffraction scanning (EBSD) analysis. Figures 3(d)–3(f) are EBSD-orientation imaging microscopy (OIM) scans, and figures 3(g)–3(i) are the corresponding inverse pole figures (IPFs) of the Sm<sub>2</sub>Co<sub>7</sub> magnets with deformations of the samples under HD70%, HD80%, and HD90%, respectively. In the OIM-EBSD map, the color of a grain specifies its orientation ac-

according to the color code. As shown in Figs. 3(d)–3(f), there are no unidentified regions in the OIM maps, indicating that all grains are  $\text{Sm}_2\text{Co}_7$  pure phase. As indicated by the color code, red represents that the grain orientation is parallel to the (001). Comparing the OIMs and their corresponding IPFs of different samples, it can be seen that the increase of deformation

is beneficial to the formation of the (001) texture. When the height reduction is 90%, the pole density of the (001) direction is 9.02, which demonstrates that the magnet of HD 90% formed a strong (001) texture, providing a higher remanence for the magnet. Good agreement is obtained among the results of hysteresis loop, XRD, and EBSD.

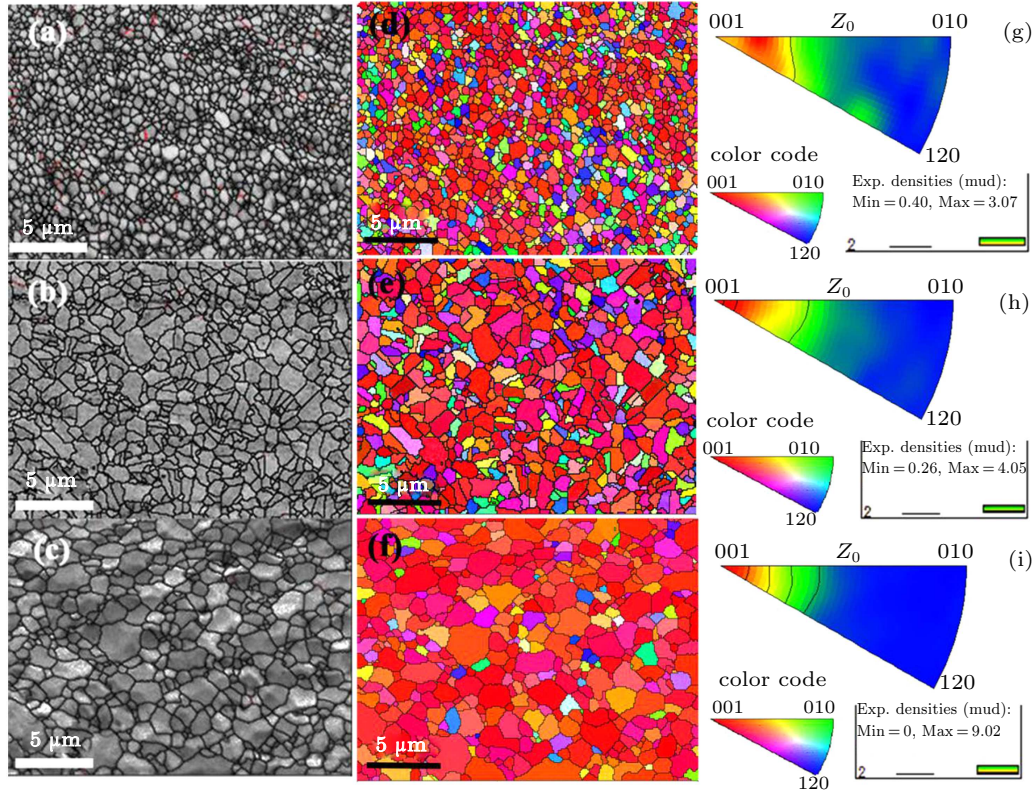


**Fig. 3.** (a)–(c) Grain size image quality (IQ) map, (d)–(f) OIM-EBSD scan, and (g)–(i) corresponding IPF of the hot deformed  $\text{Sm}_2\text{Co}_7$  magnets with 70%, 80%, and 90% height reduction, respectively.

To analyze the distribution of the orientation angle of the HD magnets, the distribution of misorientation angles was calculated and illustrated in Fig. 4. The black line in Fig. 4 shows the angular distribution of the orientation difference in the random orientation, and the histograms show the angular distribution of the orientation difference measured by the specimens. The distribution of the grain misorientation angles of the HD magnet is different from the random distribution (black line in Fig. 4), which is due to the continuous evolution of grain orientation during the deformation. The texture is strengthened with the increase of deformation degree, indicating that the concentration of grain misorientation angles is related to the texture. From Fig. 4, it can be seen that the distribution of orientation difference of the HD90% magnet is concentrated around  $30^\circ$ , while the distribution of orientation difference of the HD70% and HD80% magnets is weaker at around  $30^\circ$ . This manifests that during the HD process, the grains tend to form a concentrated orientation relationship while forming the texture, and this orientation relationship is related to the

mechanism of the texture formation of the grain rotation and recrystallization.<sup>[19–22]</sup> The results of XRD, EBSD, and misorientation analysis consistently show that the increase in deformation can promote the formation of (001) texture. Good (001) texture is primary for the permanent magnet materials to improve remanence.

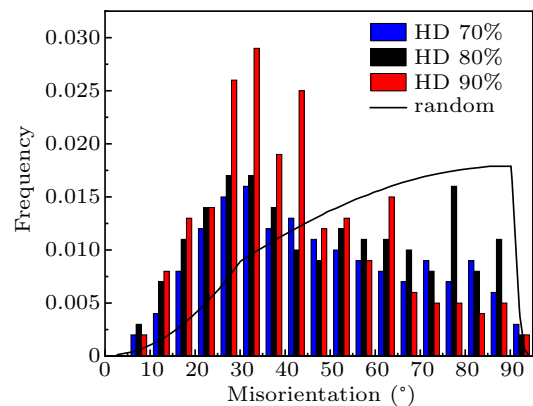


**Fig. 4.** Distribution of the grain misorientation angles of the  $\text{Sm}_2\text{Co}_7$  HD magnets.

#### 4. Conclusions and perspectives

In this study, anisotropic Sm<sub>2</sub>Co<sub>7</sub> magnets were prepared by using spark plasma sintering and hot deformation techniques. When the height reduction is 70% in the hot-deformed process, an ultra-high coercivity magnet with a coercivity of 50.68 kOe is obtained. The ultra-high coercivity is contributed to the uniform distribution of nano-scale grain size of HD70% samples. The  $M_r/M_s$ , XRD, and EBSD OIM analyses are in such a good agreement in proving that the hot deformation process can produce *c*-axis orientation texture of the Sm<sub>2</sub>Co<sub>7</sub> magnets, and the larger the deformation amount is, the better the *c*-axis texture of the magnets. And thus, the products of the Sm<sub>2</sub>Co<sub>7</sub> magnets are found acquired with higher remanence and magnetic energy. Future work will focus on the mechanism of texture evolution in Sm<sub>2</sub>Co<sub>7</sub> hot deformation magnets.

#### References

- [1] Zhang J, Takahashi Y K, Gopalan R and Hono K 2007 *J. Magn. Magn. Mater.* **310** 1
- [2] Yue M, Zhang X Y and Liu J P 2017 *Nanoscale* **9** 3674
- [3] Skokov K P and Gutflleisch O 2018 *Scr. Mater.* **154** 289
- [4] Liu Y G, Xu L, Wang Q F, Li W and Zhang X Y 2009 *Appl. Phys. Lett.* **9** 172502
- [5] Gutflleisch O, Willard M A, Brück E, Chen C H, Sankar S G and Liu J P 2011 *Adv. Mater.* **42** 821
- [6] Yue M, Li C L, Wu Q, Z H Ma, Xu H H and Palaka S 2018 *J. Chem. Eng.* **343** 1
- [7] Xu X C, Li Y Q, Ma Z H, Yue M and Zhang D T 2020 *Scripta. Mater.* **178** 34
- [8] Nakamura H 2018 *Scr. Mater.* **154** 273
- [9] Ma Z H, Liang J M, Ma W, Cong L Y, Wu Q and Yue M 2019 *Nanoscale* **11** 12484
- [10] Liu W Q, Zuo J H, Yue M, Lv W C, Zhang D T and Zhang J X 2011 *J. Appl. Phys.* **109** 07a731
- [11] Huang M Q, Wallace W E, McHenry M, Chen Q and Ma B M 1998 *J. Appl. Phys.* **83** 6718
- [12] Ma Q, Yue M, Lv W C, Zhang H G, Yuan X K, Zhang D T, Zhang X F, Zhang J X and Gao X X 2016 *J. Magn.* **21** 25
- [13] Liu S Q 2019 *Chin. Phys. B* **28** 017501
- [14] Campos M F, Yonamine T, Fukuhara M, Machado R, Romero S A, Landgraf F J G, Rodrigues D and Missell F P 2007 *J. Appl. Phys.* **101** 09
- [15] Yonamine T, Fukuhara M, Machado R and Missell F P 2008 *J. Magn. Magn. Mater.* **320** e77
- [16] Ma Q, Yue M, Xu X C, Zhang H G, Zhang D T, Zhang X F and Zhang J X 2018 *AIP. Adv.* **8** 056214
- [17] Yue M, Zuo J H, Liu W Q, Lv W C, Zhang D T, Zhang J X, Guo Z H and Li W 2011 *J. Appl. Phys.* **109** 07A711
- [18] Fang L, Zhang T, Wang H, Jiang C and Liu J 2018 *J. Magn. Magn. Mater.* **446** 200
- [19] Xu W W, Song X Y, Zhang Z X and Liang H N 2013 *Mater. Sci. Eng.* **178** B971
- [20] Sakamoto Y, Kojima S, Kojima K, Ohtani T and Kubo T 1979 *J. Appl. Phys.* **50** 2355
- [21] M. Zhu and Li W 2017 *AIP Advances* **7** 056236
- [22] Yuan X K, Yue M, Zhang D T, Jin T N, Zhang Z R, Zuo J H, Zhang J X, Zhu J and Gao X X 2014 *CrystEngComm* **16** 1669